1-1-2018

CO2 saturated brine injected into fractured shale: An X-ray micro-tomography in-situ analysis at reservoir conditions

Hongyan Yu

Yihuai Zhang

Maxim Lebedev

Zhenliang Wang

Jinfeng Ma

See next page for additional authors

10.1016/j.egypro.2018.11.021

Yu, H., Zhang, Y., Lebedev, M., Wang, Z., Ma, J., Cui, Z., ... Iglauer, S. (2018). CO2 saturated brine injected into fractured shale: An X-ray micro-tomography in-situ analysis at reservoir conditions. *Energy Procedia*, 154, 125-130. Available here

Authors

Hongyan Yu, Yihuai Zhang, Maxim Lebedev, Zhenliang Wang, Jinfeng Ma, Zhihao Cui, Michael Verrall, Andrew Squelch, and Stefan Iglauer

Available online at www.sciencedirect.com

ScienceDirect

Energy Procedia 154 (2018) 125–130

Energy Procedia

www.elsevier.com/locate/procedia

Applied Energy Symposium and Forum, Carbon Capture, Utilization and Storage, CCUS 2018, 27–29 June 2018, Perth, Australia

CO_2 saturated brine injected into fractured shale: An X-ray micro-tomography in-situ analysis at reservoir conditions

Hongyan Yu[a,b,*], Yihuai Zhang[c], Maxim Lebedev[c], Zhenliang Wang[a], Jinfeng Ma[a], Zhihao Cui[a], Michael Verrall[d], Andrew Squelch[c,e], Stefan Iglauer[f]

[a]*National & Local Joint Engineering Research Center for Carbon Capture and Sequestration Technology; Department of Geology, Northwest University, Xi'an, 710069, China*

[b]*Research Institute of BGP, CNPC, Zhuozhou 072750, China*

[c]*WA School of Mines: Minerals, Energy and Chemical Engineering, Curtin University, 26 Dick Perry Avenue, Kensington 6151, Australia*

[d]*Earth Sciences and Resource Engineering, CSIRO, 26 Dick Perry Avenue, 6151 Kensington, Australia*

[e]*Computational Image Analysis Group, Curtin Institute for Computation, Curtin University*

[f]*School of Engineering, Edith Cowan University, 270 Joondalup Drive, Joondalup 6027, Australia*

Abstract

Fracture morphology and permeability are key factors in enhanced gas recovery (EOR) and Carbon Geo-storage (CCS) in shale gas reservoirs as they determine production and injection rates. However, the exact effect of CO_2-saturated (live) brine on shale fracture morphology, and how the permeability changes during live brine injection and exposure is only poorly understood. We thus imaged fractured shale samples before and after live brine injection in-situ at high resolution in 3D via X-ray micro-computed tomography. Clearly, the fractures' aperture and connectivity increased after live brine injection.

Keywords: shale; live brine; fracture morphology; permeability

1. Introduction

Carbon capture and storage (CCS) in underground geological formations, such as depleted oil/gas reservoirs or saline aquifers is considered to be an effective approach to trap large amounts of CO_2 and thus mitigate climate warming [1-3]. CO_2 injected into sandstone [4-6], limestone [7-9] and coal seams [10-12] has been extensively

10.1016/j.egypro.2018.11.021

investigated. However, shale gas reservoirs - which contributed significantly towards energy security in the past years [13-17] - have not been systemically evaluated in this context.

The injected CO_2 is partially miscible with the resident brine [18], and reacts with the formation water to carbonic acid, thus becoming acidic [19, 20]. This CO_2-saturated (live) brine chemically reacts with the host rock [21-24]. This is particularly the case for limestone, which is significantly dissolves during live brine injection, which thus drastically increases limestone permeability [25-32]. This effect also occurs in the sandstone as some cements dissolve (such as calcite, ferrodolomite) [33-37]. It is thus clear that the acidic environment severely impacts on the micro structure and permeability of the rock.

However, no significant attention has been given to the potential structural, morphological changes in shale. We thus e imaged the shale in 3D at high resolution in-situ with X-ray micro-computed tomography before and after live brine injection to assess the micro structural characteristics and their potential changes.

2. Materials and experimental methodology

A plug (5 mm diameter and 5 mm length) was drilled out of a larger core sample from a shale gas reservoir in the Ordos basin in China. The plug was housed in an X-ray transparent high pressure unconstrained flow cell [28, 38], which was connected to an experimental core flooding apparatus built for fluid permeability measurement. The whole system was vacuumed for one day to remove all air from the system. All fluids were heated to 323 K and the core was subjected to 5 MPa effective stress. The core was then imaged by x-ray computerized micro-tomography (microCT) at a resolution of $(3.43\ \mu m)^3$. Subsequently live brine at a constant flow rate of 0.1 mL/min was injected for almost 5 hours, and the plug was microCT imaged again.

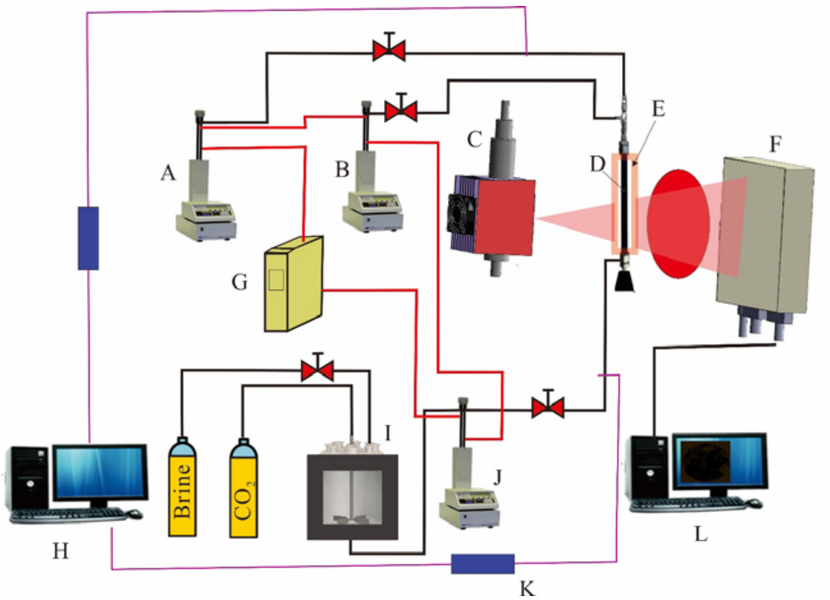

Fig. 1. (A) Injection pump, (B) Confining pump, (C) X-ray source; (D) pressurized core holder, (E) Heated tape, (F) Detector panel, (G) Water bath, (H) computer for data logging, (I) Reactor, (J) Production pump, (K) Pressure sensor, (L) CT images record computer.

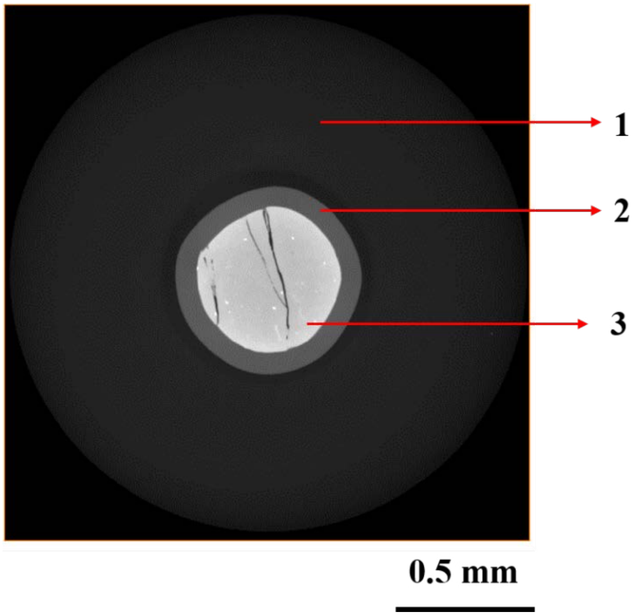

Fig. 2. Raw computerized tomography (CT) image slice showing the core holder cell (1), Teflon sleeve (2) and sample (3).

3. Results and discussion

3.1. Morphology of fracture network

The fracture network in the shale sample is visualized in Figures 3 and 4, before and after live brine injection. The black lines are the fractures, white points are high density minerals (such as pyrite and siderite), and grey is the clay mineral matrix (Figure 4). A significant change in the fractures morphology was observed before and after live flooding. Clearly, the fracture aperture increased after live brine injection, compare also Figure 5. Importantly, the fractures' connectivity also increased after live brine injection.

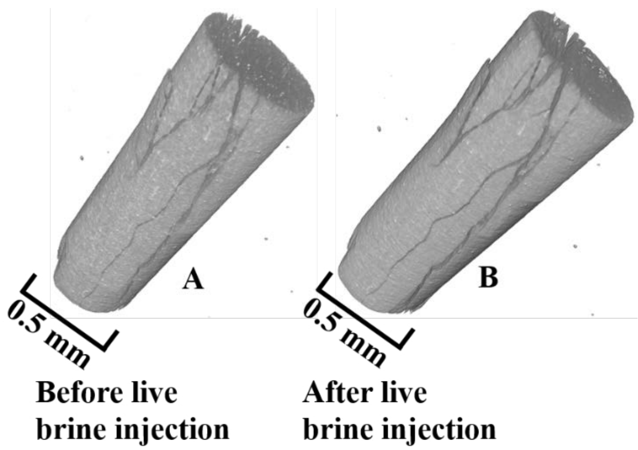

Fig. 3. 3D visualizations of the shale sample before (A) and after (B) live brine injection. The dark grey lines are the fractures, and grey is the mineral matrix.

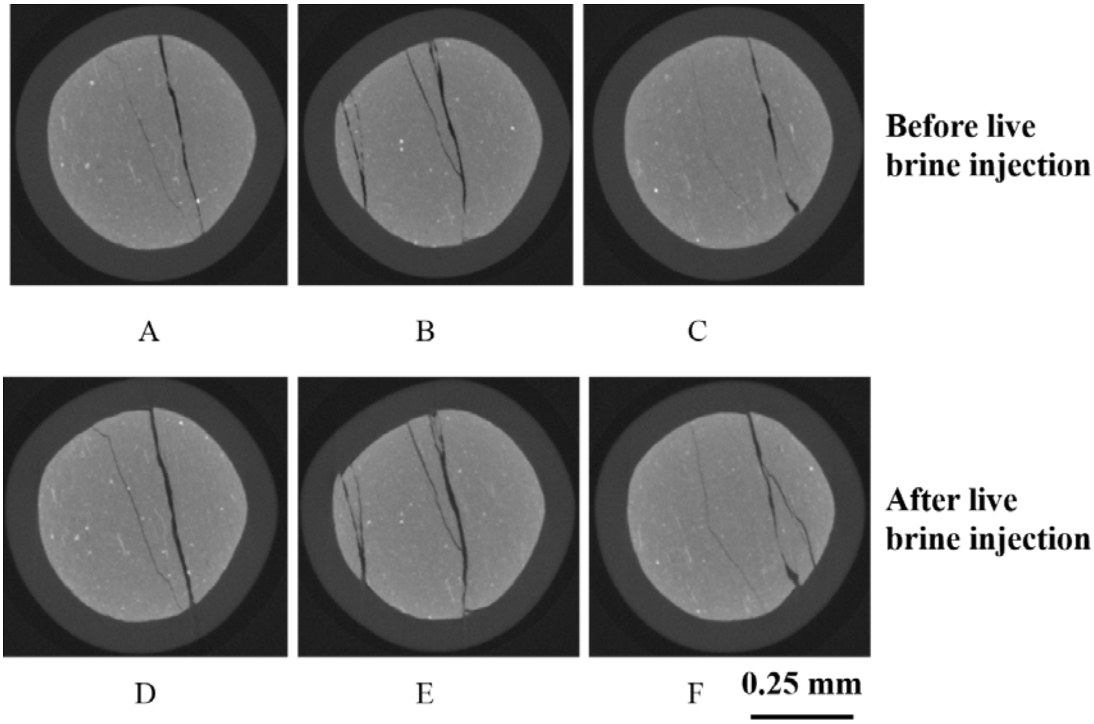

Fig. 4. 2D slices through the micro CT images of the shale sample before (a, b, c) and after (d, e, f) live brine injection.

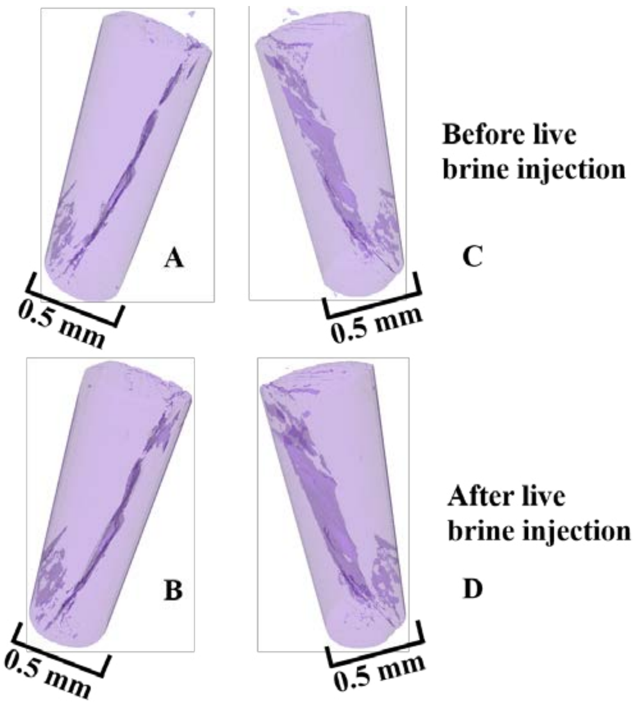

Fig. 5. Transparent 3D visualizations of the shale sample before (a, b) and after (c, d) live brine injection.

3.2. Discussion

This increase in fracture network size and connectivity after live brine injection can be interpreted as follows.

(1) the hydraulic injection pressure of the fluid opened the fractures;
(2) the acidic live brine dissolved some shale minerals, e.g. the carbonate cement [39, 40], this increased the connectivity.

4. Conclusion

Rock microstructure is an essential factor which determines CO_2 storage capacity and injectivity in shale gas reservoirs. CO_2 injected into shale gas reservoirs will cause adsorption, dissolution and molecular diffusion [15, 16, 41], which will in turn affect the microstructure.

In order to assess the possibility of the shale reservoirs geosequestration, we thus imaged a shale sample in high resolution via 3D microCT before and after 5 hrs live brine injection to investigate the change of the stress regime acting on the fractures. We observed that the fractures' apertures and fracture connectivity increased significantly after live brine injection. Hence, we conclude that CO_2 injection into shale reservoirs can cause significant morphological changes, which will affect storage efficiency.

Acknowledgements

This study was supported by the Special Fund from the State Key Laboratory of Continental Dynamics at Northwest University in China and the Donors of the Shaanxi Province Specialized Research Fund of Higher Education (Grant No. 14JK1740). The measurements were performed using the microCT system and nanoindentation system courtesy of the National Geosequestration Laboratory (NGL) of Australia. Funding for the facilities was provided by the Australian Federal Government. This work was also supported by the Pawsey Supercomputing Centre, who provided the Avizo 9.2 image processing software and workstation, with funding from the Australian Government and the Government of Western Australia.

References

[1] Samuelson, J. and C.J. Spiers, Fault friction and slip stability not affected by CO_2 storage: Evidence from short-term laboratory experiments on North Sea reservoir sandstones and caprocks. International Journal of Greenhouse Gas Control, 2012. 11: p. S78-S90.
[2] Kumar, A., et al., Reservoir simulation of CO_2 storage in aquifers. Spe Journal, 2005. 10(03): p. 336-348.
[3] Kopp, A., H. Class, and R. Helmig, Investigations on CO_2 storage capacity in saline aquifers: Part 1. Dimensional analysis of flow processes and reservoir characteristics. International Journal of Greenhouse Gas Control, 2009. 3(3): p. 263-276.
[4] Krevor, S., et al., Relative permeability and trapping of CO_2 and water in sandstone rocks at reservoir conditions. Water resources research, 2012. 48(2).
[5] Berg, S., S. Oedai, and H. Ott, Displacement and mass transfer between saturated and unsaturated CO_2–brine systems in sandstone. International Journal of Greenhouse Gas Control, 2013. 12: p. 478-492.
[6] Xu, T., et al., Numerical modeling of injection and mineral trapping of CO_2 with H2S and SO_2 in a sandstone formation. Chemical Geology, 2007. 242(3-4): p. 319-346.
[7] Mohamed, I., J. He, and H.A. Nasr-El-Din, Effect of brine composition on CO_2/limestone rock interactions during CO_2 sequestration. Journal of Petroleum Science Research, 2013.
[8] Garcia-Rios, M., et al., Influence of the flow rate on dissolution and precipitation features during percolation of CO_2-rich sulfate solutions through fractured limestone samples. Chemical Geology, 2015. 414: p. 95-108.
[9] Zhang, Y., et al. Geo-Mechanical Weakening of Limestone Due to Supercritical CO_2 Injection. in Offshore Technology Conference Asia. 2016. Offshore Technology Conference.

[10] Zhang, Y., et al., Swelling-induced changes in coal microstructure due to supercritical CO_2 injection. Geophysical Research Letters, 2016. 43(17): p. 9077-9083.
[11] Larsen, J.W., The effects of dissolved CO_2 on coal structure and properties. International Journal of Coal Geology, 2004. 57(1): p. 63-70.
[12] Busch, A. and Y. Gensterblum, CBM and CO_2-ECBM related sorption processes in coal: a review. International Journal of Coal Geology, 2011. 87(2): p. 49-71.
[13] Dahaghi, A.K. Numerical simulation and modeling of enhanced gas recovery and CO_2 sequestration in shale gas reservoirs: A feasibility study. in SPE international conference on CO_2 capture, storage, and utilization. 2010. Society of Petroleum Engineers.
[14] Jiang, J., Y. Shao, and R.M. Younis. Development of a multi-continuum multi-component model for enhanced gas recovery and CO_2 storage in fractured shale gas reservoirs. in SPE improved oil recovery symposium. 2014. Society of Petroleum Engineers.
[15] Kim, T.H., J. Cho, and K.S. Lee, Evaluation of CO_2 injection in shale gas reservoirs with multi-component transport and geomechanical effects. Applied Energy, 2017. 190: p. 1195-1206.
[16] Fernø, M., et al., Flow visualization of CO_2 in tight shale formations at reservoir conditions. Geophysical Research Letters, 2015. 42(18): p. 7414-7419.
[17] Arif, M., et al., Influence of shale-total organic content on CO_2 geo-storage potential. Geophysical Research Letters, 2017.
[18] Peng, C., Crawshaw, J.P., Maitland, G.C., Trusler, J.M. and Vega-Maza, D., 2013. The pH of CO_2-saturated water at temperatures between 308 K and 423 K at pressures up to 15 MPa. The Journal of Supercritical Fluids, 82, pp.129-137.
[19] Kaszuba, J.P., D.R. Janecky, and M.G. Snow, Experimental evaluation of mixed fluid reactions between supercritical carbon dioxide and NaCl brine: Relevance to the integrity of a geologic carbon repository. Chemical Geology, 2005. 217(3-4): p. 277-293.
[20] Rosenbauer, R.J., T. Koksalan, and J.L. Palandri, Experimental investigation of CO_2–brine–rock interactions at elevated temperature and pressure: Implications for CO_2 sequestration in deep-saline aquifers. Fuel processing technology, 2005. 86(14-15): p. 1581-1597.
[21] Hassanzadeh, H., M. Pooladi-Darvish, and D.W. Keith, Accelerating CO_2 dissolution in saline aquifers for geological storage □ Mechanistic and sensitivity studies. Energy & Fuels, 2009. 23(6): p. 3328-3336.
[22] Mojtaba, S., et al., Experimental study of density-driven convection effects on CO_2 dissolution rate in formation water for geological storage. Journal of Natural Gas Science and Engineering, 2014. 21: p. 600-607.
[23] Kneafsey, T.J. and K. Pruess, Laboratory experiments and numerical simulation studies of convectively enhanced carbon dioxide dissolution. Energy Procedia, 2011. 4: p. 5114-5121.
[24] Soong, Y., et al., Experimental and simulation studies on mineral trapping of CO_2 with brine. Energy Conversion and Management, 2004. 45(11-12): p. 1845-1859.
[25] Noiriel, C., P. Gouze, and D. Bernard, Investigation of porosity and permeability effects from microstructure changes during limestone dissolution. Geophysical research letters, 2004. 31(24).
[26] Iglauer, S., et al., Permeability evolution in sandstone due to injection of CO_2-saturated brine or supercritical CO_2 at reservoir conditions. Energy Procedia, 2014. 63: p. 3051-3059.
[27] Khather, M., et al., Experimental investigation of changes in petrophysical properties during CO_2 injection into dolomite-rich rocks. International Journal of Greenhouse Gas Control, 2017. 59: p. 74-90.
[28] Lebedev, M., et al., Carbon geosequestration in limestone: Pore-scale dissolution and geomechanical weakening. International Journal of Greenhouse Gas Control, 2017. 66: p. 106-119.
[29] Abdoulghafour, H., L. Luquot, and P. Gouze, Characterization of the mechanisms controlling the permeability changes of fractured cements flowed through by CO_2-rich brine. Environmental science & technology, 2013. 47(18): p. 10332-10338.
[30] Luquot, L., H. Abdoulghafour, and P. Gouze, Hydro-dynamically controlled alteration of fractured Portland cements flowed by CO_2-rich brine. International Journal of Greenhouse Gas Control, 2013. 16: p. 167-179.
[31] Menke, H.P., et al., Dynamic three-dimensional pore-scale imaging of reaction in a carbonate at reservoir conditions. Environmental science & technology, 2015. 49(7): p. 4407-4414.
[32] Al-Khdheeawi, E.A., et al., Effect of wettability heterogeneity and reservoir temperature on CO_2 storage efficiency in deep saline aquifers. International Journal of Greenhouse Gas Control, 2018. 68: p. 216-229.
[33] Rahman, T., et al., Residual trapping of supercritical CO_2 in oil-wet sandstone. Journal of colloid and interface science, 2016. 469: p. 63-68.
[34] Al-Yaseri, A., et al., Permeability Evolution in Sandstone Due to CO_2 Injection. Energy & Fuels, 2017. 31(11): p. 12390-12398.
[35] Sarmadivaleh, M., A.Z. Al-Yaseri, and S. Iglauer, Influence of temperature and pressure on quartz–water–CO_2 contact angle and CO2–water interfacial tension. Journal of colloid and interface science, 2015. 441: p. 59-64.
[36] Iglauer, S., et al., CO_2 wettability of caprocks: Implications for structural storage capacity and containment security. Geophysical Research Letters, 2015. 42(21): p. 9279-9284.
[37] Iglauer, S., et al., Residual CO_2 imaged with X-ray micro-tomography. Geophysical Research Letters, 2011. 38(21).
[38] Iglauer, S. and M. Lebedev, High pressure-elevated temperature x-ray micro-computed tomography for subsurface applications. Advances in Colloid and Interface Science, 2017.
[39] Shao, H., J.R. Ray, and Y.-S. Jun, Dissolution and precipitation of clay minerals under geologic CO_2 sequestration conditions: CO_2− brine− phlogopite interactions. Environmental science & technology, 2010. 44(15): p. 5999-6005.
[40] Angeli, M., et al., Experimental percolation of supercritical CO_2 through a caprock. Energy Procedia, 2009. 1(1): p. 3351-3358.
[41] Li, X. and D. Elsworth, Geomechanics of CO_2 enhanced shale gas recovery. Journal of Natural Gas Science and Engineering, 2015. 26: p. 1607-1619.